



Design, synthesis, and evaluation of some metal ion complexes of mannich base derived from 2-Mercaptobenzimidazole as potential antimicrobial agents

Thuraya Q. Sabah^a, Shaymaa R. Baqer^{a,*}

^a Department of Chemistry, College of Science for Women, University of Baghdad, Baghdad, Iraq

Abstract

This study aims to prepare new compounds and investigate them spectroscopically and biologically against selected types of positive and negative bacteria and fungi to demonstrate their biological effectiveness. The prepared ligand combining formaldehyde, indole, sulfa benzamide, and 2-mercapto benzimidazole, a Mannich base ligand (L) was synthesized. The six metal ions including Cobalt (II), Nickel (II), Copper (II), Palladium (II), Platinum (IV), and gold (III) have interacted with the ligand and formed new complexes. Different spectroscopic methods, including C.H.N.S., FTIR, UV- Range visible, ¹HNMR, ¹³CNMR, mass spectra, magnetic moment, and molar conductivity were used to suggest the new geometry of the complexes. The result from the infrared spectrum showed that the ligand behaves as tridentate with all prepared complexes. Conductivity analysis revealed the electrolytic nature of palladium, platinum, and gold ions complexes and non-electrolytes. The antibacterial activity of the compounds that were produced was tested using an agar-well diffusion procedure towards two strains of gram-positive as well as two strains of gram-negative bacteria and fungi (*Staphylococcus*, *Streptococcus*, *Escherichia coli*, *Pseudomonas aeruginosa*, and *Candida albicans*) respectively at 0.02M. The standard (ΔE°) and (ΔH_f°) of ligand and six complexes were calculated using the program Hyper chem 8.0.7. The research established that complexes are more stable than ligands. Calculated HOMO and LUMO and vibration frequencies using (parametric method 3 (PM3)) to find out the active sites in the ligand showed that they can coordinate and note the extent to which the results of theoretical vibrational frequencies are close to the process when calculating the vibrational frequency of the active aggregates.

Keywords: Complexes of Transition Metals; Mannich Base; 2-Mercaptobenzimidazole; Sulfa benzamide; Antibacterial and anti-fungal.

Received on 13/11/2023, Received in Revised Form on 06/01/2024, Accepted on 06/01/2024, Published on 30/09/2024

<https://doi.org/10.31699/IJCPE.2024.3.13>

1- Introduction

Heterocyclic compounds are compounds that contain different atoms other than the hydrogen atom. Heterocyclic compounds are cyclic organic substances that are composed of one or more of the elements nitrogen, oxygen, and sulfur [1, 2]. To obtain benzimidazole, a heterocyclic aromatic chemical compound, a benzene ring is fused with an imidazole ring at the (4,5) location. Throughout the resonance process [3], the inclusion of a benzene ring in a benzimidazole improves the resonance systems, which raises the benzimidazole molecule's stability [4]. Mannich revealed the very first "Mannich-base," which unified two separate chemical units over a CH₂ methylene bridge [5, 6]. Because of the many interactions of these molecules, Mannich's base was crucial to the advancement of synthetic organic chemistry [7]. They may easily be transformed into a range of novel chemicals and are highly reactive and valuable intermediates in synthetic chemistry [8, 9]. The medicinal properties of Mannich base derivatives have been reported to include

antibacterial, anticonvulsant [10], anti-inflammatory, antioxidant [11], and anti-Alzheimer effects [12].

Due to their sensitivity and selectivity to metal ions, Mannich bases' metal complexes have recently received attention. There are numerous medical and biological uses for Mannich-based complexes, including antibacterial, antifungal, anti-tuberculosis, antiulcer [13], and anticancer [14]. This study aims to prepare new compounds (ligands and complexes with different metal elements. After diagnosing them and deducing their shape, they were studied biologically against different types of negative and positive bacteria and fungi and compared with a standard drug to demonstrate the biological importance of the prepared compounds.

2- Experimental work

An Eager 300 elemental analyzer was utilized to determine (carbon, hydrogen, nitrogen, and sulfur). Shimadzu atomic absorption 670 Flam spectrophotometer was used to determine the metal content. A WTW conduct meter at 25 °C was used to measure the conductance values in 10⁻³ M in a solution of all prepared



*Corresponding Author: Email: shaimaarb_chem@csw.uobaghdad.edu.iq

© 2024 The Author(s). Published by College of Engineering, University of Baghdad.

This is an Open Access article licensed under a [Creative Commons Attribution 4.0 International License](https://creativecommons.org/licenses/by/4.0/). This permits users to copy, redistribute, remix, transmit and adapt the work provided the original work and source is appropriately cited.

complexes. Shimadzu and Perkin Elmer FT-IR spectrophotometers were used to measure the vibration frequencies by using KBr and CsI particles. The absorbance of all prepared compounds was detected in ethanol solution in the UV-visible region using a spectrophotometer (Shimadzu UV-Vis. 1800 PC). The ^1H , ^{13}C -NMR data was acquired with DMSO for a solvent and TMS as an internal reference on a Fourier transform

Varian spectrometer operating at 500 MHz. The magnetic susceptibility of each compound was measured at 25 °C by the balance of Johnson Matthey. All produced compounds' melting temperatures were identified using the Gallen Kamp M.F.B-60. The GC-Mass measurement was carried out using the US-made 5973 network mass selective detector. Several chemicals with high purity were used in this research which are listed in Table 1.

Table 1. Chemical Formula, State, and Purity of All Compounds Used

NO.	CHEMICAL COMPOUNDS	CHEMICAL FORMULA	STATE	PURITY %	NAME OF COMPANY
1	Chloroplatinic acid hexahydrate	$\text{H}_2\text{PtCl}_6 \cdot 6\text{H}_2\text{O}$	SOLID	99	G; ENTHAM LIFE SCIENCES
2	Cobalt chloride hexahydrate	$\text{CoCl}_2 \cdot 6\text{H}_2\text{O}$	SOLID	99	BDH
3	Copper chloride dehydrate	$\text{CuCl}_2 \cdot 2\text{H}_2\text{O}$	SOLID	99	BDH
4	Formaldehyde	HCOH	LIQUID	99	C.D.H
5	Ethanol	$\text{C}_2\text{H}_6\text{O}$	LIQUID	99	C.D.H
6	hydrogen tetrachloride aurate (III) trihydrate	$\text{HAuCl}_4 \cdot 3\text{H}_2\text{O}$	SOLID	98	G; ENTHAM LIFE SCIENCES
7	Palladium chloride	PdCl_2	SOLID	99	C.D.H
8	2-Mercaptobenzimidazol	$\text{C}_7\text{H}_6\text{N}_2\text{S}$	SOLID	98	Ratnam and Bio
9	Indole	$\text{C}_8\text{H}_7\text{N}$	SOLID	99	Merck.
10	Sulfa benzamide	$\text{C}_{13}\text{H}_{12}\text{N}_2\text{O}_3\text{S}$	SOLID	99	TEMD CO.
11	Nickel chloride hexahydrate	$\text{NiCl}_2 \cdot 6\text{H}_2\text{O}$	SOLID	99	BDH
12	Chromium (III) chloride hexahydrate	$\text{CrCl}_3 \cdot 6\text{H}_2\text{O}$	SOLID	99	C.D.H

2.1. Formation of the starting material (2-(1H endol-1-yl) methyl thio)-1H benzo[d]imidazole(S)

0.75 g of 0.005 mol 2-mercaptobenzimidazol was dissolved in 5 ml of absolute ethanol. Then, 0.585 g of 0.005 mol indole and 2 drops of hydrochloric acid were added. After complete dissolution, the mixture was placed in an ice bath in a round flask. 0.5 ml of formaldehyde was added after 5 min. The mixture was placed in a round flask with stirring by refluxed method for 6 h. A mixture of distilled water and ethanol was used to wash the bright orange precipitate which was dried, and the melting point was recorded at 229-231 °C [15].

2.2. Synthesis of N-(4-((2-((1H-indol-1-yl) methylthio)-1H-benzo[d]imidazole-1-yl) methylamino) phenylsulfonyl) benzamide(L)

In a round bottom flask, 0.84 g of 0.003 mol of S was dissolved in 5 ml absolute ethyl alcohol. After complete dissolution, 0.5 ml of formaldehyde in an ice bath and 0.82 g of 0.003 mol sulfabenzamide were dissolved in ethanol with 1 drop of HCl in the presence of heat and stirring using the refluxed method for 6 h. Then, the mixture was left to dry. The mixture was kept overnight in the refrigerator. The ligand (L) was formed, recrystallized using ethanol, and filtered to produce a precipitate with a light purple color, see Fig. 1. The melting point of the Mannich compound was 164-165 °C, yield of 76%, and a molecular formula of $\text{C}_{30}\text{H}_{26}\text{N}_5\text{O}_3\text{S}_2$ (L). The main steps of the synthesis of Mannich base (L) are shown in Fig. 1.

2.3. Synthesis of ligand complexes

Mannich base L was formed by reacting equal moles of the ligand and the metal ion in an ethyl alcohol solvent in

a 250 ml round flask. In another round flask, a combined mole of $\text{CoCl}_2 \cdot 6\text{H}_2\text{O}$ salt was dissolved using a glass stirrer. The total capacity was 100 ml, followed by a new addition of the ligand. Different colors were shown depending on the utilized metal ion. The mixture was heated for 3 h at 50 °C under constant stirring, and then the precipitate was allowed to dry. The crystallization was completed with ethanol. This process was carried out with a variety of metal ions including nickel (II), copper (II), palladium (II), platinum (IV), and gold (III).

2.4. Parameters were estimated as a part of a theoretical treatment using the Hyperchem 8.0.7 program and parametric method 3 (PM3)

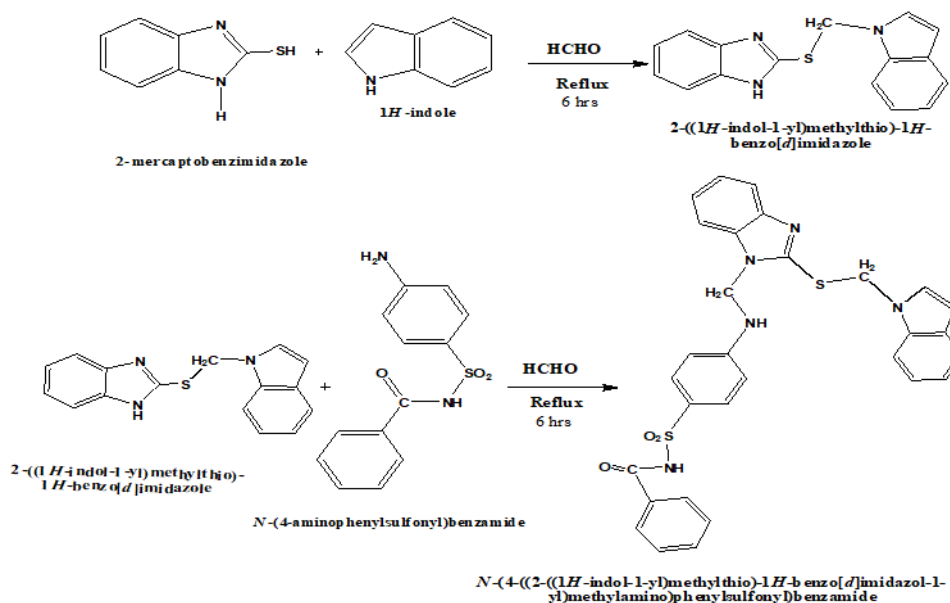
- 1- Standard (ΔE°) and (ΔH_{f0}) for formed ligands and complexes
- 2- Highest and lowest occupied molecular orbitals for ligands
- 3- Vibration frequencies of the infrared spectrum for ligands.

2.5. Activity against fungi and bacteria

The good diffusion method was utilized for evaluating the efficiency of ligands and their metal complexes versus pathogenic microorganisms according to aerobic circumstances. 40 g of culture medium for bacteria and fungi were dissolved in a liter of distilled water. This combination was used as a culture material for bacteria (*Escherichia coli*, *Streptococcus*, *Staphylococcus aureus*, *Pseudomonas aeruginosa*), (*Agar Mueller Hinton*), and for fungi, *Candida albicans* (*Sabouraud Dextrose Agar*). After melting by heating, the culture medium was placed in the autoclave for 15 minutes, then it was poured into sterile plastic dishes and left to solidify. A hole was made using a cork drill with a diameter of 6 mm to add the substance that inhibits the growth of bacteria and fungi.

The prepared ligands and complexes were dissolved in DMSO at a concentration of 0.02M and injected into the culture medium pits. The plates were placed in the incubator at 37 °C for 24 h for antibacterial activity and

72 h for antifungal activity. The diameters of inhibition were measured using a ruler in millimeters of the prepared compounds.



3- Results and discussion

The prepared complexes were obtained in the form of colored precipitates. The analysis of all data for ligand (L) and metal complexes is summarized in Table 2. An organic ethanol solvent was used in the preparation of all metallic complexes. The analytical data suggested a ratio

of 1:1 for all complexes. The ligand and their metal complexes were characterized depending on the results of the element analysis, infrared spectra, UV-vis spectra, mass spectra, ¹H and ¹³C nuclear magnetic resonance spectra, magnetic susceptibility, and conductivity for prepared complexes.

Table 2. Physical Properties of Compounds

Formula MWt	m.p ^o C	Color	Yield%	Elemental analysis Calc.				Metal% Calc.
				(Found)				(Found)
				C	H	N	S	
C ₃₀ H ₂₆ N ₃ O ₃ S ₂ (L) 567.68	164-165	Light Purple	76	63.46 (64.04)	4.58 (5.21)	12.33 (11.73)	11.29 (12.11)	-----
C ₃₀ H ₂₉ N ₃ O ₅ S ₂ Co 733.49	152-155	Red-brown	67	49.08 (48.67)	3.95 (3.54)	9.54 (9.00)	8.74 (9.02)	10.38 (11.21)
C ₃₀ H ₂₉ O ₅ N ₃ S ₂ Ni 733.25	Over300	Brown	69	49.09 (49.49)	3.95 (4.24)	9.54 (10.11)	8.74 (9.33)	8.00 (7.58)
C ₃₀ H ₂₉ O ₅ S ₂ Cu 738.1	288-290	Dark brown	73	48.77 (47.89)	3.92 (4.81)	9.48 (9.99)	8.68 (9.22)	8.60 (9.52)
C ₃₀ H ₂₅ N ₃ O ₃ S ₂ Pd 745.1	160-162	Dark black	71	48.32 (49.11)	3.35 (4.13)	9.39 (10.38)	8.60 (7.88)	14.28 (15.03)
C ₃₀ H ₂₅ O ₃ N ₃ S ₂ Pt 904.5	198-200	Light pink	77	39.80 (38.88)	2.76 (3.7)	7.58 (8.44)	6.95 (7.04)	21.14
C ₃₀ H ₂₅ N ₃ O ₃ S ₂ Au 870.99	143-145	Pink	81	41.33 (42.21)	2.57 (3.00)	8.03 (8.67)	7.36 (7.89)	22.61 (23.18)

3.1. Fourier transform infrared spectroscopy

The number of functional groups that are important in diagnosis appeared in the ligand spectrum. Some important bands at [ν_{NH} , ν_{CS} , ν_{CSC} , $\nu_{\text{CH}_2\text{N}}$] which were due to (3286, 3352, 1199, 754, 2897 and 2966) cm^{-1} sequentially [16, 14], see Fig. 2. When coordination to the nitrogen atom of NH group, methylene group of Mannich base and sulfur atoms of CS group a red or blue shift occurs in the peaks of these complexes with change

in the shape of the bands and it coordinated as tridentate ligand with all the six selected ions cobalt, nickel, copper, palladium, platinum and gold complexes. The imine, SO₂, and CO bands which appeared at frequencies 1597, 1037, 1153 and 1681 cm^{-1} did shift in all the prepared complexes, which indicates that it was not involved in coordination [17]. Further appearance of medium bands at 563-559, 478-447, and 345-310 cm^{-1} were related to $\nu_{\text{M-N}}$, $\nu_{\text{M-S}}$, and $\nu_{\text{M-Cl}}$ in all complexes which confirms the occurrence of coordination

through it [18, 19]. Table 3 shows additional bands were performed. It is also observed that the water absorption

bands in the outer and inner sphere coordination can be observed in Table 3, Fig. 2, Fig. 3, and Fig. 4.

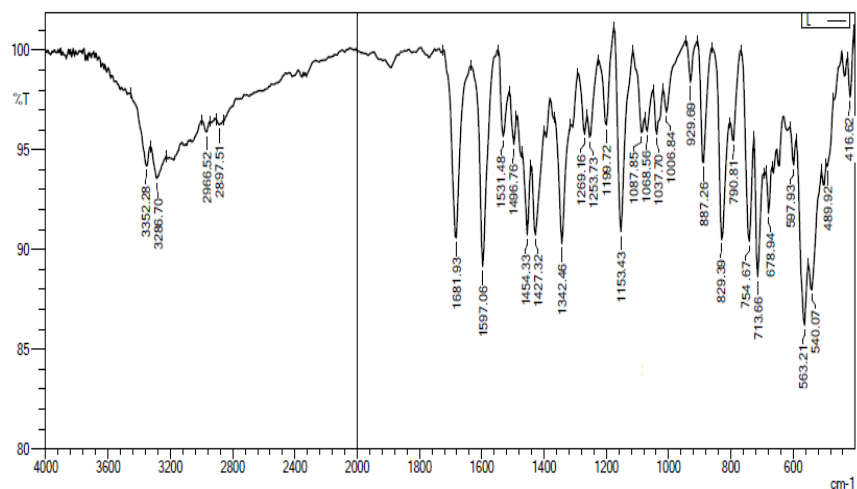


Fig. 2. Infrared Spectrum of Ligand (L)

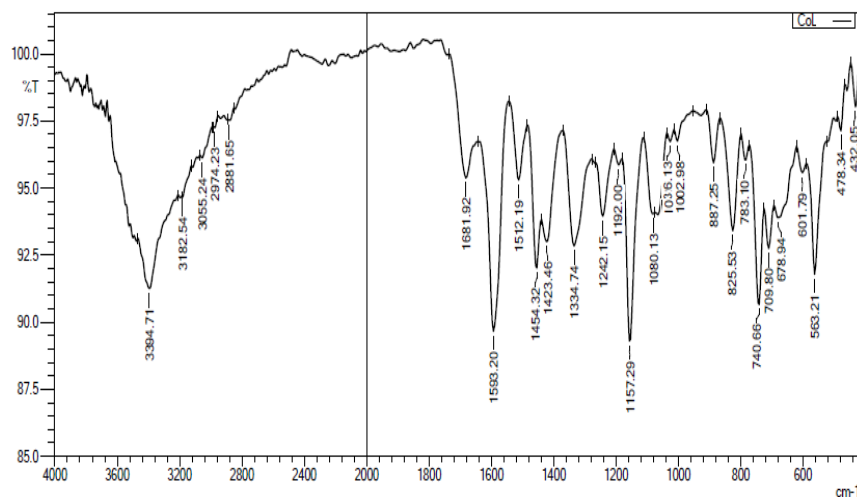


Fig. 3. Infrared Spectrum of CoL

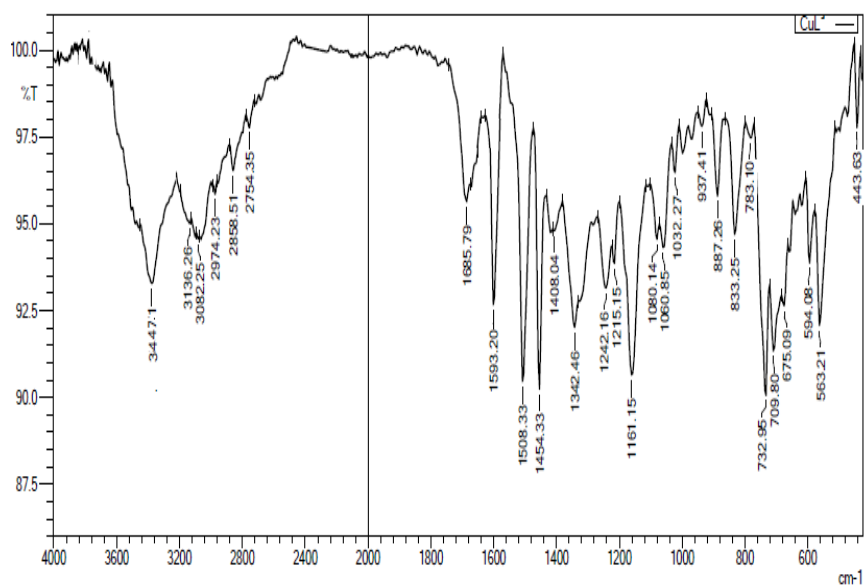


Fig. 4. Infrared Spectrum of CuL

Table 3. Fourier Transforms Spectroscopy (FT-IR) Of Functional Group of Mannich igand (L), And Their Metal Complexes

Comp.	$\nu\text{C=O}$	$\nu\text{C=N}$ ring	νNH	νSO_2	νCSC	νCS	$\nu\text{CH}_2\text{-N}$	$\nu\text{M-N}$	$\nu\text{M-S}$	$\nu\text{M-Cl}$	H_2O bands
L	1681	1597	3286 3352	1037 1153	1199	754	2897 2966	-----	-----	-----	----
[Co(L)Cl ₂ H ₂ O]. H ₂ O	1681	1593	3182	1036 1157	1192	740	2881 2974	563	478	337	3394 1512 783
[Ni(L)Cl ₂ H ₂ O].H ₂ O	1685	1597	3155 3357	1038 1153	1190	740	2877 2978	563	493	321	3502 1512 786
[Cu(L)Cl ₂ H ₂ O]. H ₂ O	1685	1593	3136	1032 1161	1215	732	2858 2974	563	443	345	3447 1508 783
Pd(L)Cl] Cl	1681	1593	3250	1034 1157	1238	740	2839 2958	563	478	310	-----
Pt (L) Cl ₃] Cl	1685	1597	3271 3352	1032 1153	1189	744	2854 2924	563	420	345	-----
Au(L)Cl] Cl ₂	1685	1593	3147	1032	1189	744	2823	559	447	320	-----

3.2. Ultra-violet transitions, magnetic and conductivity properties

The Uv-vis spectra of the ligand and metal ion complexes were examined in ethyl alcohol around 25 °C. Table 4 shows the electronic spectra information for all produced compounds. In the Mannich ligand, the band in the region 25510-27247 cm⁻¹ is attributed to the n → π* transition which reflects the ligand's nonbonding electrons. Another band at 44843 cm⁻¹ is attributed to π → π* transition.

(a) In cobalt complex, bands appeared at 10893, 19607, and 23041 cm⁻¹ are assigned to ⁴T_{1g} → ⁴T_{2g}, ⁴T_{1g} → ⁴A_{2g(F)}, and ⁴T_{1g} → ⁴T_{1g(P)} transitions due to octahedral geometry of Co (II) [20]. An additional band that appeared at 30769 cm⁻¹ is related to the intra-Ligand → CoCT. Magnetic-moment 3.93 B.M. In the DMF, the conductivity recorded of 12 μS.cm⁻¹ showed the complex was non-ionic [21]. According to this outcome, the complex was high in the electronic spectrum of the complex as shown in Table 4. Fig. 5 shows the geometry of the cobalt complex.

(b) In nickel complex, bands appeared at 10728, and 18115 cm⁻¹ are assigned to ³A_{2g} → ³T_{2g}, and ³A_{2g} → ³T_{1g} transitions according to the order and forbidden band at 13661 cm⁻¹ due to ³A_{2g} → ¹E_g. This transition indicates the octahedral geometry of Ni [19, 20]. Additional bands that appeared at 32258, 3101, and 40816 cm⁻¹ are related to the intra ligand → NiCT. Magnetic moment 3.18 B.M. In the DMF, the conductivity recorded of 14 μS.cm⁻¹ showed the complex was non-ionic [21]. The electronic spectrum of this complex can be seen in Table 4. Fig. 5 shows the geometry of the nickel complex.

(c) In the copper complex, a band that appeared at 12135 cm⁻¹ is assigned to ²E_g → ²T_{2g}, and 31446, 35971, and

46728 cm⁻¹ are related to the intra Ligand → CuCT. Magnetic moment 1.85 B.M. This transition indicates an octahedral geometry of Copper (II) [22]. The complex was nonionic (μS.cm⁻¹) [23]. According to this outcome, the complex was dark-brown paramagnetic and high-spin oct. The electronic spectrum of the complex can be seen in Table 4. Fig. 5 shows the geometry of a copper complex.

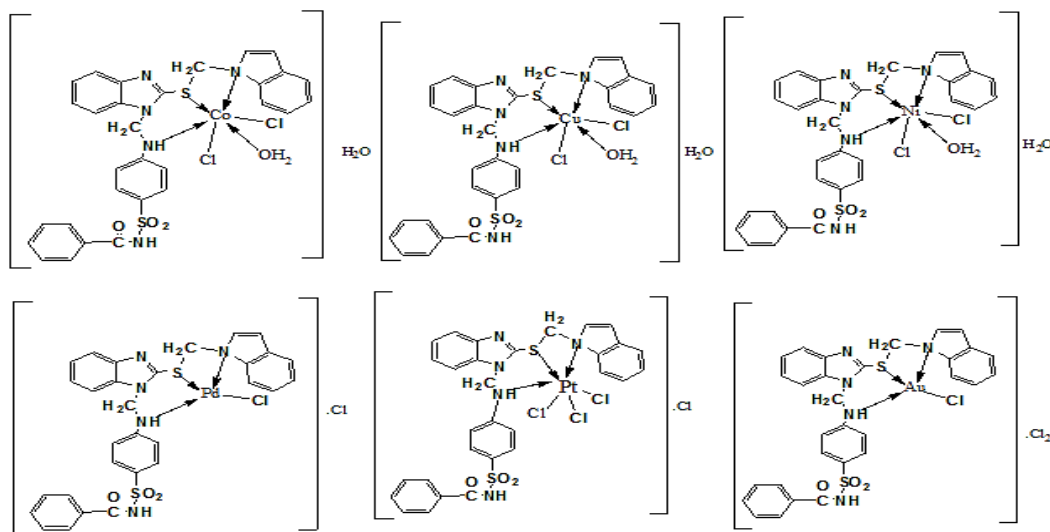
(d) Inpalladium (II)complex, bands appeared at 22522, 25839 cm⁻¹ is assigned to ¹A_{1g} → ¹B_{1g}, ¹A_{1g} → ¹E_g transitions according to the order. A band that appeared at 25839 cm⁻¹ is related to the intra Ligand → PdCT. Magnetic-moment (0) B.M. which indicates the square-planer geometry of this complex [24]. This value shows that the complex was low spin 77 μS.cm⁻¹ confirming the complex was ionic [25]. The square planer complex has diamagnetic properties. The electronic spectrum of this complex can be seen in Table 4. Fig. 5 shows the geometry of the palladium complex.

(f) In platinum (IV) complex, bands appeared at 20703 and 28703 cm⁻¹ are assigned to ¹A_{1g} → ¹T_{1g} and ¹A_{1g} → ¹T_{2g}, transitions according to the order which indicates octahedral geometry of Pt (IV) [24]. The forbidden band at 12091 cm⁻¹ is assigned to ¹A_{1g} → ³T_{2g}. Magnetic moment 0 B.M. This value indicates that the complex was low spin. In the DMF, the recorded conductivity of 82 μS.cm⁻¹ indicates that the complex was ionic [26].

(g) In pink gold (III) complex, bands appeared at 28571 and 23041 cm⁻¹ are assigned to ¹A_{1g} → ¹B_{1g}, and ¹A_{1g} → ¹E_g transitions according to the order which indicate square planer geometry Au (III) Magnetic-moment 0 B.M. [27]. The recorded conductivity of 142 μS.cm⁻¹ indicates the complex was ionic [28]. Fig. 5 shows the geometry of the gold complex.

Table 4. The Conductivity in DMF, Electronic Spectra, Magnetic of Complexes, and Suggested Geometrical Structures for Ligand and Their Metal Complexes

Comp.	Absorption nm.	Absorption cm-	Assignment	μ_{eff} B.M. found (calculated)	Conductivity ($\mu\text{s.cm}^{-1}$)	Suggested Geometry
L	392	25510	$n \rightarrow \pi^*$	-----
	367	27247	$n \rightarrow \pi^*$			
	223	44843	$\pi \rightarrow \pi^*$			
CoL	918	10893	${}^4T_{1g} \rightarrow {}^4T_{2g}$	3.93 (3.87)	12	Octahedral
	510	19607	${}^4T_{1g} \rightarrow {}^4A_{2g(f)}$			
	434	23041	${}^4T_{1g} \rightarrow {}^4T_{1g(p)}$			
	325	30769	IntraLigand \rightarrow NiCT			
NiL	932	10728	${}^3A_{2g} \rightarrow {}^3T_{2g}$	3.18 (2.82)	14	Octahedral
	730	13661	${}^3A_{2g} \rightarrow {}^1E_g$			
	552	18115	${}^3A_{2g} \rightarrow {}^3T_{1g}$			
	310	32258	IL \rightarrow NiCT			
	277	36101	IL \rightarrow NiCT			
CuL	824	12135	${}^2E_g \rightarrow {}^3T_{2g}$	1.80 (1.73)	18	Octahedral
	318	31446	IL \rightarrow CuCT			
	278	35971	IL \rightarrow CuCT			
	214	46728	IL \rightarrow CuCT			
PdL	444	22522	${}^1A_{1g} \rightarrow {}^1B_{1g}$	0.00	77	Square planar
	387	25839	${}^1A_{1g} \rightarrow {}^1E_g$			
	305	32786	IL \rightarrow PdCT			
PtL	827	12091	${}^1A_{1g} \rightarrow {}^3T_{2g}$	0.00	82	Octahedral
	483	20703	${}^1A_{1g} \rightarrow {}^1T_{2g}$			
	348	28735	IL \rightarrow PtCT			
	315	31746	IL \rightarrow PtCT			
AuL	299	33444	IL \rightarrow PtCT	0.00	145	Square planar
	350	28571	${}^1A_{1g} \rightarrow {}^1B_{1g}$			
	434	23041	${}^1A_{1g} \rightarrow {}^1E_g$			
	222	45045	IL \rightarrow AuCT			

**Fig. 5.** The Proposed Geometry of the Formed Complexes

3.3. NMR spectra

Another way to identify ligands is proton nuclear resonance spectroscopy. The chemical shifts indicated by ${}^1\text{H-NMR}$ in the ligand spectrum are seen in Table 5. The spectrum of the free Mannich-base (L) shows a singlet absorption peak appeared at δ peak at $\delta 8.03$ and 12.27 ppm equivalent to one proton that assigned to (N-H) the secondary amine beside methylene and carbonyl group respectively [29]. Another multiple proton peaks between

$\delta 7.23$ and 7.90 that belong to Ar-H aromatic present in the ligands $\delta 5.61$, 5.73 , and $\delta 5.83, 5.91$. These bands refer to methylene groups of Mannich base [30]. Another peak can be seen in Table 5. The spectrum of ${}^{13}\text{CNMR}$ of L appeared at 168.4 ppm indicating the carbon of carbonyl group. The signals observed between $110.38-133.44$ ppm are due to C-Ar aromatic phenyl ring and $53.06, 56.64$ ppm for (the methylene group), another signal which appeared at 165.73 ppm was due to the C-NH group. There are other peaks which can be seen in Table 5.

Table 5. ^1H and ^{13}C NMR of Mannich Base Ligand (L)

Functional groups	$^1\text{HNMR}$ δ ppm	Functional groups	$^{13}\text{CNMR}$ δ ppm
DMSO (solvent)	2.52	DMSO (solvent)	39.09-40.75
H ₂ O	3.54	C-NH	165.73
Ar-H	7.23- (7.90,17, H, multiplet)	C-Ar	110.38-133.44
CH ₂ -N (Mannich) groups	2 (5.61,5.73,2H Duplet) (5.83,5.91,2H Duplet)	CH ₂ -N (Mannich) 2 groups	(53.06,56.64)
N-H beside Mannich group	(8.03,1H, singlet)	C=N of benzimidazole ring	150.96
NH beside carbonyl group	(12.27,1H, Singlet)	C=O group	168.64

3.4. Mass spectra

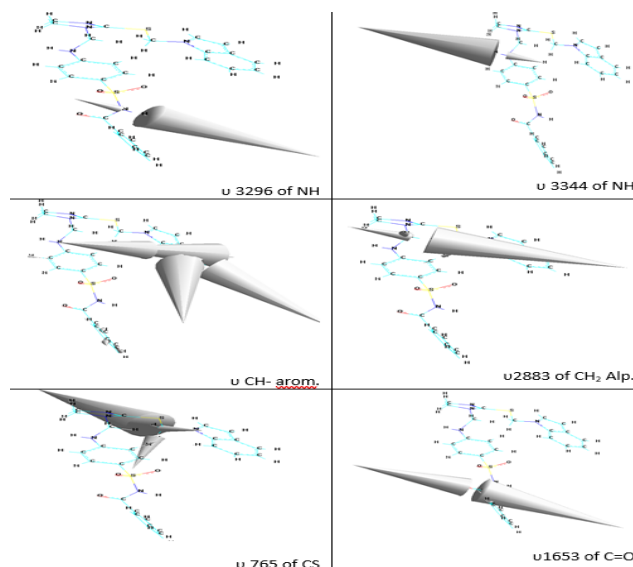
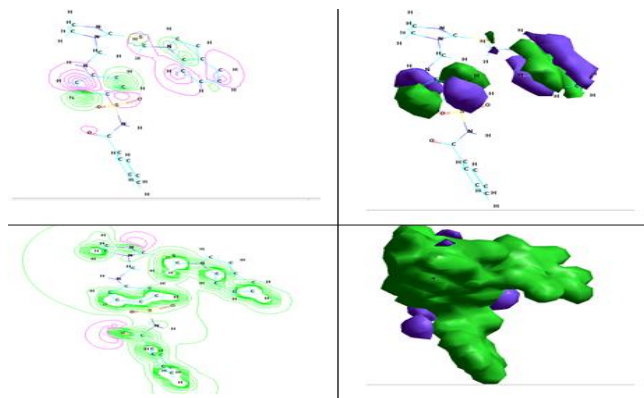
The mass spectrum of N-(4-((2-((1H-indol-1-yl)methylthio)-1H-benzo[d]imidazole-1-yl)methylamino)phenylsulfonyl)benzamide (L) was detected. Fig. 2 shows an insignificant intensity peak at $m/z = 567.5$, which occurred by the molecular ion of the empirical formula. ($\text{C}_{30}\text{H}_{25}\text{N}_5\text{O}_3\text{S}_2$). The fragment peak at $162\ m/z$ [$(\text{C}_8\text{H}_6\text{N}_2\text{S})^+, 100$] represents the base peak. Other fragments peak at $437\ m/z$ [$(\text{C}_{22}\text{H}_{17}\text{N}_4\text{O}_3\text{S}_2)^+, 55$], $275\ m/z$ [$(\text{C}_{13}\text{H}_{11}\text{N}_2\text{O}_3\text{S})^+, 15$], $155\ m/z$ [$(\text{C}_6\text{H}_5\text{NO}_2\text{S})^+, 38$], $130\ m/z$ [$(\text{C}_9\text{H}_8\text{N})^+, 42$], $120\ m/z$ [$(\text{C}_7\text{H}_6\text{NO})^+, 40$], $78\ m/z$ [$(\text{C}_6\text{H}_6)^+, 42$], $43\ m/z$ [$(\text{CHNO})^+, 28$] can be seen in Fig. 5.

3.5. Theoretical Computation Vibration Frequencies of Ligand

Using the PM3 method provides greater compatibility with experimental information than other methods. The vibration spectrum of the ligand L was estimated using this method and the results can be seen in Fig. 6. HOMO and LUMO was calculated for the ligand molecule to show the active groups in it and the binding sites as shown in Fig. 7, where the electron density locations and the probability of binding occurred through it. In the PM3 method, the heat of formation and binding energy were calculated for cobalt, nickel, and copper complexes and complexes of palladium, platinum, and gold using the AMBER method. Complexes were more stable than ligands, based on the results obtained as shown in Table 6.

Table 6. Heat of Formation and Binding Energy (ΔHf° and ΔE°) By Two Methods PM3 and amber

Comp.	PM3		AMBER
	ΔHf°	ΔE°	$\Delta\text{E}^\circ = \Delta\text{Hf}^\circ$
L	85.7908	-7536.3761994	-----
CoL	-206123.4230661	-6273.7999339	-----
NiL	-23132.8899974	-6345.0830026	-----
CuL	-49802.950321	-7877.98604	-----
PdL	-----	-----	94.4444
PtL	-----	-----	251.7626
AuL	-----	-----	69.5861

**Fig. 6.** Vibration Spectrum of Mannich Base Ligand (L)**Fig. 7.** HOMO and LUMO of Ligand (L)

3.6. Antibacterial and antifungal activity

The results obtained regarding Mannich ligand base L and accompanying novel complexes' antibacterial and antifungal properties are shown in Table 7. All dishes' inhibitory diameters were acquired in millimeters. The antibacterial and antifungal action of all complexes prepared were estimated in contrast to certain gram-positive and gram-negative microorganisms, (*Staphylococcus*, *streptococcus*, *Escherichia coli*, *pseudomonasaeruginosa*), and *candidaalbicans* fungi at concentration 0.02 M using the standard drug (amoxicillin) with bacteria and fluconazole standard

antifungal drug as shown in Fig. 8. The results showed that the ligand is more effective than the standard drug and complexes with all types of selected bacteria except for the copper complex. Where the copper complex showed high effectiveness against selected bacteria except

E-Coli and with fungi higher than the other prepared complexes. Regarding the fungi, the findings revealed that the ligand and all prepared compounds had greater activity than the standard medication except for the platinum complex which had a low inhibition zone [27].

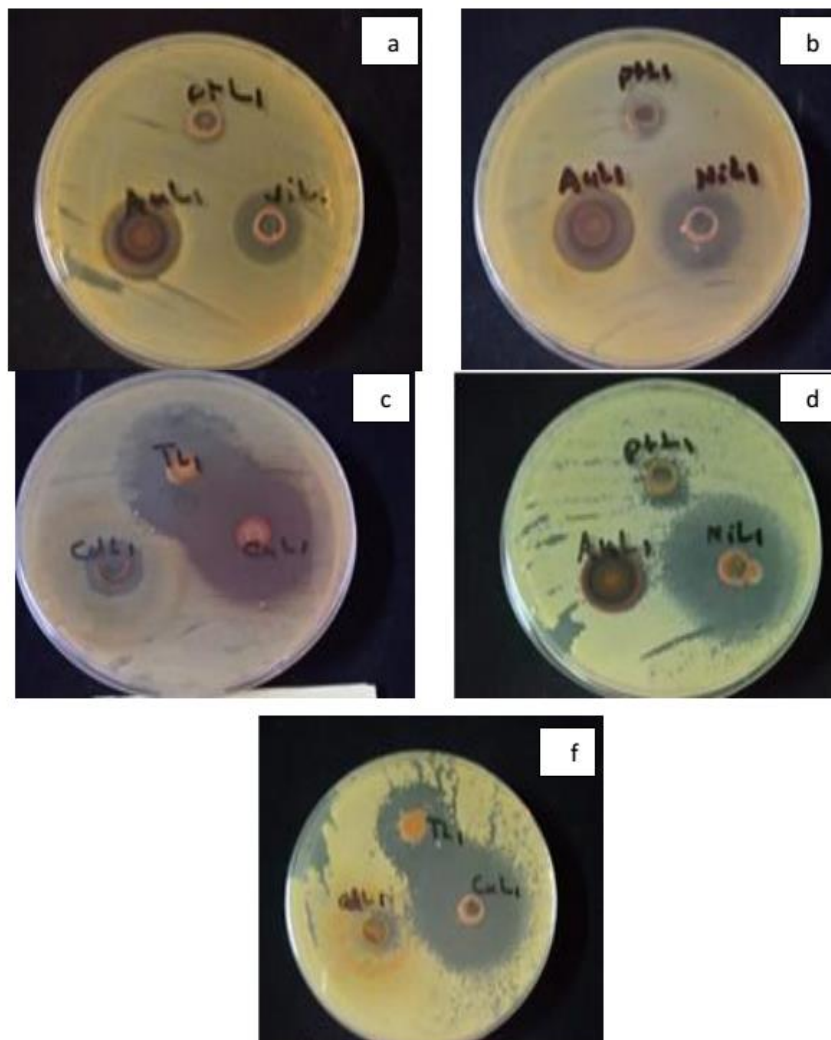


Fig. 8. Bacteria and fungi dishes and inhibition zone when (a): *pseudo monasaeruginosa*, (b): *Escherichiacoli*, (c): *streptococcus*, (d): *candida albicans*, (f): *candidaalbicans*

Table 7. Anti-bacterial and Antifungal Effects of All Prepared Compounds at 0.02 M

Compounds	Types of bacteria and				Fungi
	<i>Staphylococcus</i>	<i>Streptococcus</i>	<i>Escherichia coli</i>	<i>Pseudomonas aeruginosa</i>	<i>Candida albicans</i>
1 CoL	14	15	14	15	14
2 NiL	26	15	28	25	34
3 CuL	32	33	30	35	32
4 PdL	24	24	25	25	29
5 PtL	10	10	12	10	11
6 AuL	28	19	27	27	18
7 DMSO	(-)	(-)	(-)	(-)	(-)
8 L	30	32	33	29	26
9 Amoxicillin	10	9	10	9	---
10 Fluconazole	-----				12

(-) means there is no inhibition zone with the DMSO solvent

4- Conclusions

This research work includes the synthesis of a new ligand derived from 2-mercaptobenzimidazole and six coordination complexes with light and heavy metal ions of different oxidation states. Most of the spectroscopic methods were used in the diagnosis, including mass spectra, ¹HNMR, ¹³CNMR, UV-Vis, FT-IR, conductivity and magnetic moment, CHNS, and atomic absorption. The evaluation of the indication demonstrated that the six complexes have two geometry structures: octahedral with cobalt(II), nickel(II), copper(II) and platinum(IV), and square planar with palladium(II) and gold(III). The results of biological activity in general revealed that the ligand has an antibacterial activity that is higher than the standard drug and the complexes prepared with the exception of the complex with fungi. All compounds were more effective than the standard drug with the exception of the platinum complex.

References

- [1] T. Y. Fonkui, M. I. Ikhile, P. B. Njobeh, and D. T. Ndinteh, 'Benzimidazole Schiff base derivatives: synthesis, characterization, and antimicrobial activity', *BMC Chemistry.*, vol. 13, no. 1, pp. 1–11, 2019, <https://doi.org/10.1186/s13065-019-0642-3>
- [2] E. Alterhoni, A. Tavman, M. Hacioglu, O. Sahin, and A. S. B. Tan, 'Synthesis, structural characterization and antimicrobial activity of Schiff bases and benzimidazole derivatives and their complexes with CoCl₂, PdCl₂, CuCl₂ and ZnCl₂', *Journal of Molecular Structure.*, vol. 1229, p. 129498, 2021, <https://doi.org/10.1016/j.molstruc.2020.129498>
- [3] S. V. Kumar, M. R. Subramanian, and S. K. Chinnaiyan, 'Synthesis, characterization and evaluation of N-mannich bases of 2-substituted Benzimidazole derivatives', *Journal of Young Pharmacists.*, vol. 5, no. 4, pp. 154–159, 2013, <https://doi.org/10.1016/j.jyp.2013.11.004>
- [4] M.I. Khan, A. Khan , I.Hussain , M. A. Khan , S. Gul , M. Iqbal , I. Rahman , F. Khud 'Spectral, XRD, SEM and biological properties of new mononuclear Schiff base transition metal complexes', *CommunInorganic Chemistry Communications.*, vol. 35, pp. 104–109, 2013, <https://doi.org/10.1016/j.inoche.2013.06.014>
- [5] S. K. Raju, P. Vengadhajalaphathy, R. Sundaram, S. Periyasamy, T. Chinnaraj, and P. Sekar, 'Recent advances in biological applications of mannich bases—An overview', *International Journal of Pharmaceutical Chemistry and Analysis*, vol. 10, pp 15-27, 2023, <https://doi.org/10.18231/j.ijpca.2023.004>
- [6] Z. Šindelávr and P. Kopel, 'Bis (benzimidazole) Complexes, Synthesis and Their Biological Properties: A Perspective', *Inorganics*, vol. 11, no. 3, p. 113, 2023, <https://doi.org/10.3390/inorganics11030113>
- [7] A. Raduck , M. Świątkowski ,I.K.-Główniak ,B. Kaproń,T. Plech , M. Szczesio, K. Gobis,M. I. S.-Jóźwik , A. Czyłkowska,'Zinc Coordination Compounds with Benzimidazole Derivatives: Synthesis, Structure, Antimicrobial Activity and Potential Anticancer Application', *International Journal of Molecular Sciences.*, vol. 23, no. 12, p. 6595, 2022, <https://doi.org/10.3390/ijms23126595>
- [8] H. K. Mohammed and M. K. Rasheed, 'Synthesis of benzimidazole and mannich bases derivatives from 4-methyl ortho phenylenediamine and evaluation of their biological activity', *International Journal of Drug Delivery Technology.*, vol. 11, no. 2, pp. 423–428, 2021.
- [9] K. Chakrabarti, M. Maji, and S. Kundu, 'Cooperative iridium complex-catalyzed synthesis of quinoxalines, benzimidazoles and quinazolines in water', *Green Chemistry Journal.*, vol. 21, no. 8, pp. 1999–2004, 2019, <https://doi.org/10.1039/c8gc03744b>
- [10] C. Zalaru ,F.Dumitrascu ,C.Draghici , I. Tarcomnicu, M. Marinescu , G. M. Nitulescu ,R. Tatia,L. Moldovan , M. Popa , M. Carmen Chifiriuc , 'New pyrazolo-benzimidazole Mannich bases with antimicrobial and antibiofilm activities', *Antibiotics*, vol. 11, no. 8, p. 1094, 2022, <https://doi.org/10.3390/antibiotics11081094>
- [11] A. Farooq , M. Imran , Z. Iqbal ,T. H. Bokhari, S. Latif , M. Liaqat,L. Mitu., 'Synthesis, structural and photo-physical studies of transition metal complexes with Mannich bases derived from 2-mercaptobenzimidazole', *Bulletin of the Chemical Society of Ethiopia.*, vol. 32, no. 3, pp. 481–490, 2018, <https://doi.org/10.4314/bcse.v32i3.7>
- [12] C. Tian, X. Qiang, Zhongcheng Cao, C. Ye, Y.He, Y. Deng,L.Zhang., 'Flurbiprofen-chalcone hybrid Mannich base derivatives as balanced multifunctional agents against Alzheimer's disease: Design, synthesis and biological evaluation', *Bioorganic Chemistry.*, vol. 94, p. 103477, 2020, <https://doi.org/10.1016/j.bioorg.2019.103477>
- [13] T. M. Al-Mouamin and D. J. Alkhakani, 'Synthesis of New Nucleoside Analogues from Benzimidazole and Evaluation of Their Antimicrobial Activity', *Baghdad Science Journal*, vol. 13, no. 2.2 NCC, p. 317, 2016, <https://doi.org/10.21123/bsj.2016.13.2.2NCC.0317>
- [14] M. Alias and S. R. Bakir, 'Synthesis, Spectroscopic Characterization and in Vitro Cytotoxicity Assay of Mropholine Mannich Base Derivatives of Benzimidazole with Some Heavy Metals', *Al-Nahrain Journal of Science.*, vol. 21, no. 3, 2018, <http://doi.org/10.22401/JNUS.21.3.06>
- [15] M. R. Ahamed, S. F. Narren, and A. S. Sadiq, 'The Preparation of some New Mannich and Schiff bases derived from 2-Mercaptobenzimidazole', *Baghdad Science Journal*, vol. 12, no. 3, pp. 516–526, 2015, <https://doi.org/10.21123/bsj.2015.12.3.516-526>

- [16] A. Tavman, M. Hacıoglu, D. Gürbüz, A. Cinarlı, M. A. F. Oksüzömer, and A. S. B. Tan, 'Spectral characterization and antimicrobial activity of some transition metal complexes of 2-(5-nitro-1H-benzimidazol-2-yl)-4-bromophenol', *Bulletin of the Chemical Society of Ethiopia.*, vol. 33, no. 3, pp. 451–466, 2019, <https://doi.org/10.4314/bcse.v33i3.6>
- [17] H. A. Bayoumi, A.-N. M. A. Alaghaz, and M. S. Aljahdali, 'Cu (II), Ni (II), Co (II) and Cr (III) complexes with N2O2-chelating schiff's base ligand incorporating azo and sulfonamide moieties: spectroscopic, electrochemical behavior and thermal decomposition studies', *Int. J. Electrochem. Sci.*, vol. 8, no. 7, pp. 9399–9413, 2013, [https://doi.org/10.1016/S1452-3981\(23\)12979-8](https://doi.org/10.1016/S1452-3981(23)12979-8)
- [18] J. B. Bhagyasree, H. Varghese, C. Y. Panicker, J. Samuel, C.V. Alsenoy, K. Bolelli, I. Yildiz, E. Aki, 'Vibrational spectroscopic (FT-IR, FT-Raman, 1H NMR and UV) investigations and computational study of 5-nitro-2-(4-nitrobenzyl) benzoxazole', *Spectrochimica Acta Part A: Molecular and Biomolecular Spectroscopy.*, vol. 102, pp. 99–113, 2013, <https://doi.org/10.1016/j.saa.2012.09.032>
- [19] K. J. Al-Adilee, S. H. Jawad, H. A. K. Kyhoiesh, and H. M. Hassan, 'Synthesis, characterization, biological applications, and molecular docking studies of some transition metal complexes with azo dye ligand derived from 5-methyl imidazole', *Journal of Molecular Structure.*, p. 136695, 2024, <https://doi.org/10.1016/j.molstruc.2023.136695>
- [20] M. S. Refat, S. B. Bakare, T. A. Altalhi, K. Alam, and G. H. Al-Hazmi, 'Synthesis and spectroscopic interpretations of Co (II), Ni (II) and Cu (II) decycolate complexes with molecular docking of COVID-19 protease', *Polish Journal of Chemical Technology.*, vol. 23, no. 2, pp. 54–59, 2021, <https://doi.org/10.2478/pjct-2021-0017>
- [21] Ghassan Faisal Mohsin, Wasan J. Al-Kaabi, Azaldeen Kazal Alzubaidi, Describing Polymers Synthesized from Reducing Sugars and Ammonia Employing FTIR Spectroscopy', *Baghdad Science Journal.*, vol. 19, p. 6, 2022, <https://doi.org/10.21123/bsj.2022.6527>
- [22] A. A. Aldabagh and A. G. M. Al-Daher, 'Synthesis and Characterization of New Co (II), Ni (II), Cu (II) and Zn (II) with Bis-hydrazones Complexes', *Rafidain Journal of Science.*, vol. 28, no. 2, pp. 112–119, 2019, <https://doi.org/10.33899/RJS.2019.159981>
- [23] S. S. Hassan, N. M. Hassan, S. R. Baqer, and others, 'Biological evaluation and theoretical study of bi-dentate ligand for amoxicillin derivative with some metal ions', *Baghdad Science Journal.*, vol. 18, no. 4, p. 1269, 2021, <http://doi.org/10.21123/bsj.2021.18.4.1269>
- [24] F. A. I. Al-Khodir, H. Abumelha, T. Al-Warhi, S. A. Al-Issa, and others, 'New platinum (IV) and palladium (II) transition metal complexes of s-triazine derivative: synthesis, spectral, and anticancer agents studies', *BioMed Research International.*, vol. 2019, 2019, <https://doi.org/10.1155/2019/9835745>
- [25] I. H. Ibraheem, A. S. Sadiq, M. Al-Tameemi, and M. F. Alias, 'Synthesis, Spectral Identification, Antibacterial Evaluation and Theoretical Study of Co, Fe, Rh and Pd Complexes for 2-benzoylthiobenzimidazol', *Baghdad Science Journal.*, vol. 19, no. 6, p. 1326, 2022, <https://doi.org/10.21123/bsj.2022.6704>
- [26] S. R. Baqer and S. A. Alsaheb, 'Synthesis and Biological Study of Some Transition Metal Ions Complexes of Schiff-Mannich Base Derived from 2-Amino-5-', *Journal of Medicinal and Chemical Sciences.*, vol. 6, pp. 789–802, 2023, <https://doi.org/10.26655/JMCHEMSCI.2023.4.10>
- [27] N. A. Hasan and Sh.R.Baqer, Preparation, Characterization, Theoretical and Biological Study of new Complexes with mannich base , 2chloro -N (Piperidin -1-ylmethylthio)-1, 3, 4- Thiadiazol-2-yl)acetamide, *Ibn Al-Haitham Journal for Pure and Applied Sciences.* vol. 36 no. 1, 2023, <https://doi.org/10.30526/36.1.2983>
- [28] M. F. Alias and F. S. Jaafer, 'Microwave Assisted Synthesis, Solution State, Spectral Studies and Theoretical Treatment of Pd (II), Pt (IV) and Au (III) ions Complexes Containing 2-Benzamide Benzothiazole', *Baghdad Science Journal.*, vol. 12, no. 3, pp. 527–535, 2015, <https://doi.org/10.21123/bsj.2015.12.3.527-535>
- [29] Z. Zeng, G. Kociok-Kohn, T. J. Woodman, M. G. Rowan, and I. S. Blagbrough, 'The 1H NMR Spectroscopic Effect of Steric Compression Is Found in [3.3. 1] Oxa-and Azabicycles and Their Analogues', *ACS Publications Omega*, vol. 6, no. 19, pp. 12769–12786, 2021, <https://doi.org/10.1021/acsomega.1c01093>
- [30] M. Marinescu M. Marinescu, L. Otilia Cintează, G. I. Marton, M.C. Chifiriuc, M. Popa, I. Stănculescu, C.M. Zălaru & C. E. Stavarache, 'Synthesis, density functional theory study and in vitro antimicrobial evaluation of new benzimidazole Mannich bases', *BMC Chem.*, vol. 14, no. 1, pp. 1–16, 2020, <https://doi.org/10.1186/s13065-020-00697-z>

تصميم وتحضير وتقييم بعض معقدات ايونات المعادن لقاعدة مانخ المشتقة من ٢- مركبتوبنزميدازول كعوامل محتملة مضادة للميكروبات

ثرثا قفس صبا؁ شفمء راب باقر^١

^١ قسم الكفمفاء؁ كلية العلوم للنباء؁ جامعة بغداد؁ بغداد؁ العراق

الخلاصة

تهدف هذه الدراسة إلى تحضير مركبات جديدة ودراسها طيفيا بالاضافة الى دراستها بيولوجيا ضد أنواع مختارة من البكتيريا والفطريات الموجبة والسالبة لبيان مدى أهميتها فيما إذا كانت مركبات فعالة بيولوجيا ام لا. تم تحضير الليكاند من تفاعل الفورمالديهايد؁ والسلفابنزاميد و٢-مركبتوبنزميدازول والاندرول؁ حضرت قاعدة مانخ (L). تم تفاعل أيونات المعادن الستة وهي الكوبالت (II)؁ والنيكل (II)؁ والنحاس (II)؁ والبلاديوم (II)؁ والبلاتين (IV)؁ والذهب (III) مع الليكاند لتكوين معقدات جديدة. تم استخدام طرق طيفية مختلفة؁ بما في ذلك UV-VIS؁ FTIR؁ C.H.N.S.؁ ¹HNMR؁ ¹³CNMR؁ طيف الكتلة؁ العزم المغناطيسي؁ والتوصيل المولاري؁ والتي تم استخدامها لاقتراح الشكل الهندسي الجديد للمعقدات. أظهرت نتيجة طيف الأشعة تحت الحمراء أن الليكاند يسلك كليكاند ثلاثي السن مع جميع المعقدات المحضرة. أظهرت نتائج التوصيلية الطبيعية الالكتروليتيية في معقدات أيونات البلاديوم والبلاتين والذهب وغير الالكتروليتيية في البقية. تم اختبار النشاط المضاد للبكتيريا للمركبات التي تم إنتاجها على سطح الآجار تجاه سلالتين من البكتيريا موجبة بالإضافة إلى سلالتين من البكتيريا سالبة والفطريات *Staphylococcus, Streptococcus, Escherichia coli, Pseudomonas aeruginosa* and *Candida albicans* عند ٠,٠٢ مولاري. تم حساب (ΔE^0) و (ΔHf^0) للمركبات والمعقدات الستة باستخدام برنامج Hyper chem8.0.7. وأثبتت الدراسة أن المعقدات أكثر استقرارًا من الليكاند. تم حساب ترددات الاهتزاز HOMO و LUMO باستخدام طريقة PM3 لمعرفة المواقع النشطة في المجاميع القادرة على التناسق وملاحظة مدى اقتراب نتائج الترددات الاهتزازية النظرية من العملية عند حساب التردد الاهتزازي للموجات الاهتزازية والمجاميع النشطة.

الكلمات الدالة: معقدات العناصر الانتقالية؁ قواعد مانخ؁ ٢-مركبتوبنزميدازول؁ سلفابنزاميد؁ مضادات البكتيريا والفطريات.